

Towards the CO2Image mission: performance studies using AVIRIS-NG

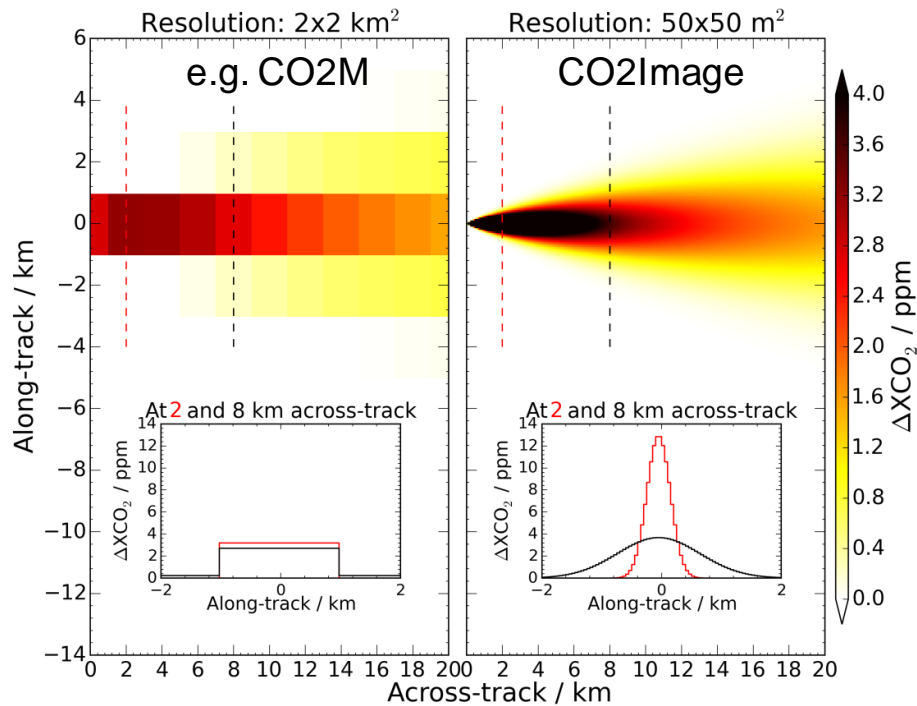
Jonas Wilzewski^{1,2}, Johan Strandgren^{1,4}, Andreas Baumgartner¹, Peter Haschberger¹, Claas Köhler¹, David Krutz¹, Carsten Paproth¹, John W. Chapman⁵, David R. Thompson⁵, Andrew K. Thorpe⁵, Bernhard Mayer², Anke Roiger¹, and André Butz³

April 30, 2021



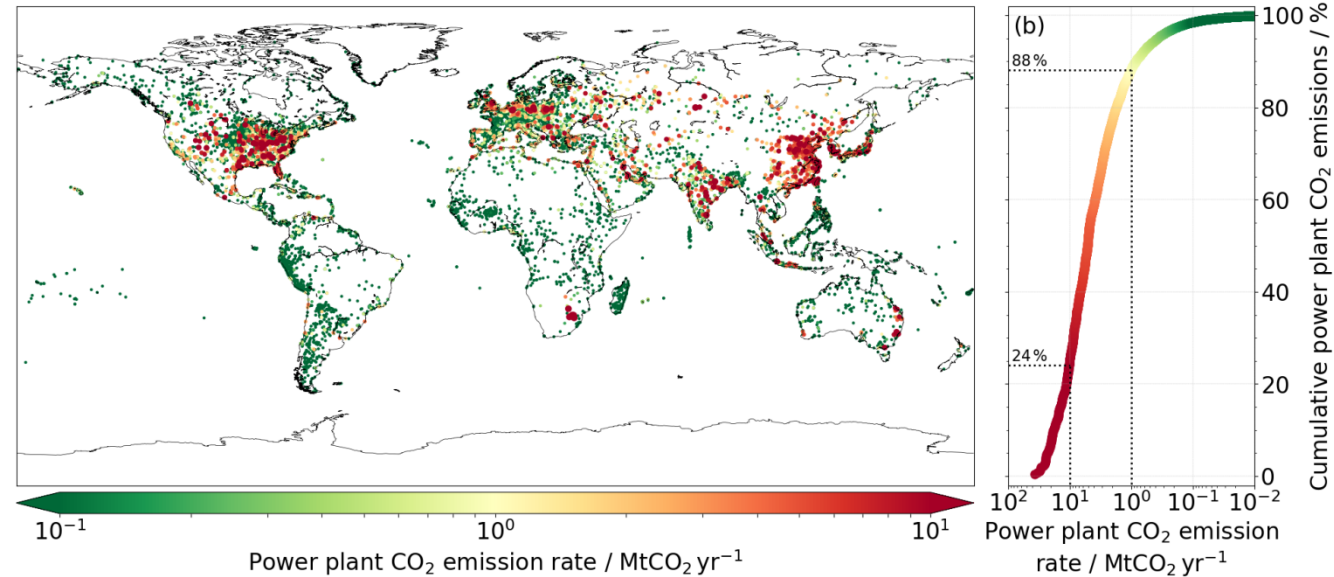
Drop by my [Zoom video call](#) after the break-out chat session to discuss with me!
(Meeting-ID: 930 6329 4310 Pwd: 749099)

The CO2Image demonstrator: a compact CO₂ monitoring sensor at 50 x 50 m² spatial resolution



[Wilzewski et al. \(2020\)](#)

- Very high spatial resolution entails coarse spectral resolution for sufficient SNR.
- Ideal spectral resolution at $\Delta\lambda = 1.3$ nm in the SWIR spectral range



[Strandgren et al. \(2020\)](#)

- Simulations show that the planned sensor can be expected to resolve plumes of medium-sized power plants (≥ 1 MtCO₂ y⁻¹).

Phase A successfully finished, launch envisaged for 2025 (DLR CompSat programme)

Retrieval performance studies with AVIRIS-NG

Goal

Use AVIRIS-NG measurements of power plant plumes to inform CO₂ emission monitoring techniques in preparation of the CO2Image demonstrator mission

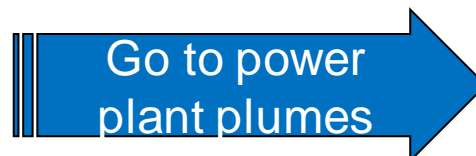
AVIRIS-NG^[1]

- Air-borne Sensor
- $\Delta\lambda \sim 5 \text{ nm}$
- $380 \text{ nm} < \lambda < 2,510 \text{ nm}$
- Observations of power plants^[2]

→ *Which spectral range / retrieval configuration is suitable to retrieve the column-averaged dry-air mole fraction of CO₂ (XCO₂) from AVIRIS-NG spectra?*

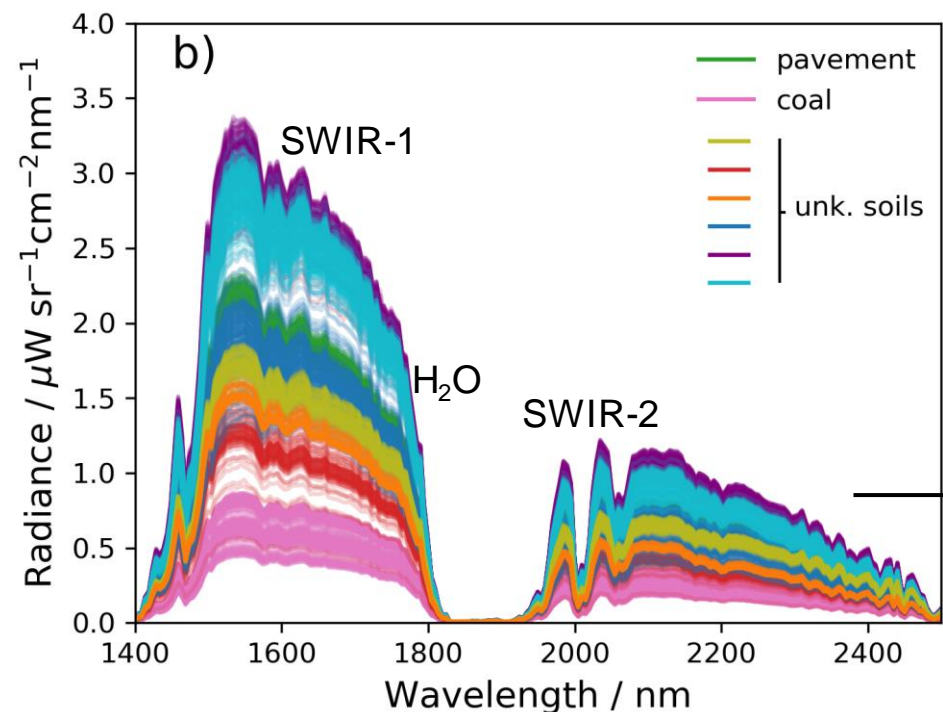
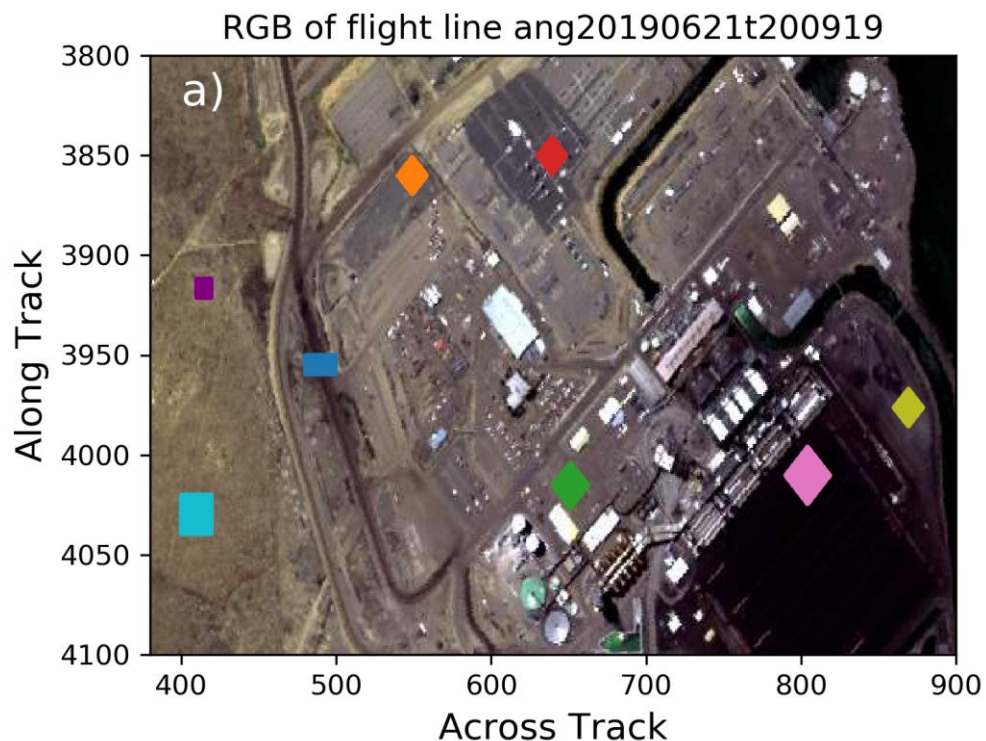


→ *Which steps are needed to estimate power plant emission rates?*



Retrieval performance studies with AVIRIS-NG

- Identification of an **ensemble of test spectra** composed of background spectra covering various surfaces



Retrieval tests carried out with the RemoTeC algorithm [\[3\]](#)[\[4\]](#)

Retrieval state vector

- [CO₂]
- [H₂O]
- Spectral baseline polynomial → albedo
- Spectral shift

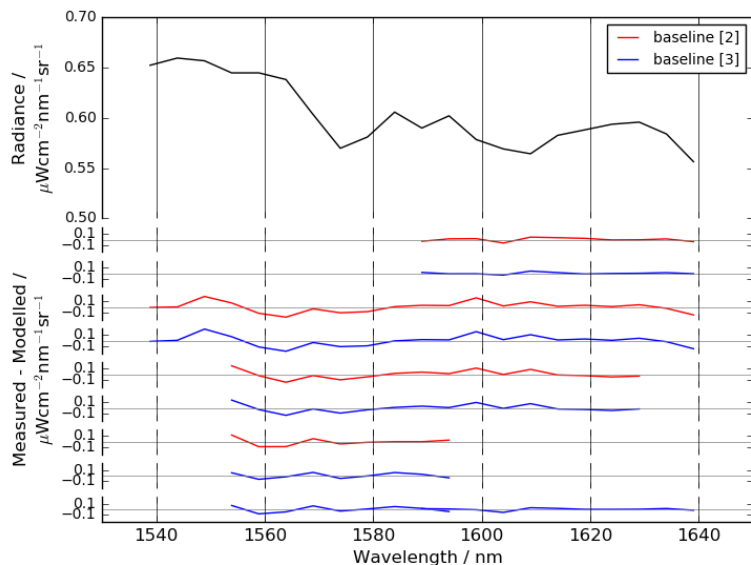
a) True color image of AVIRIS-NG measurement in New Mexico, USA

b) Background spectra selected from the colored shapes in a) to test the XCO₂ retrievals (N=1,369)

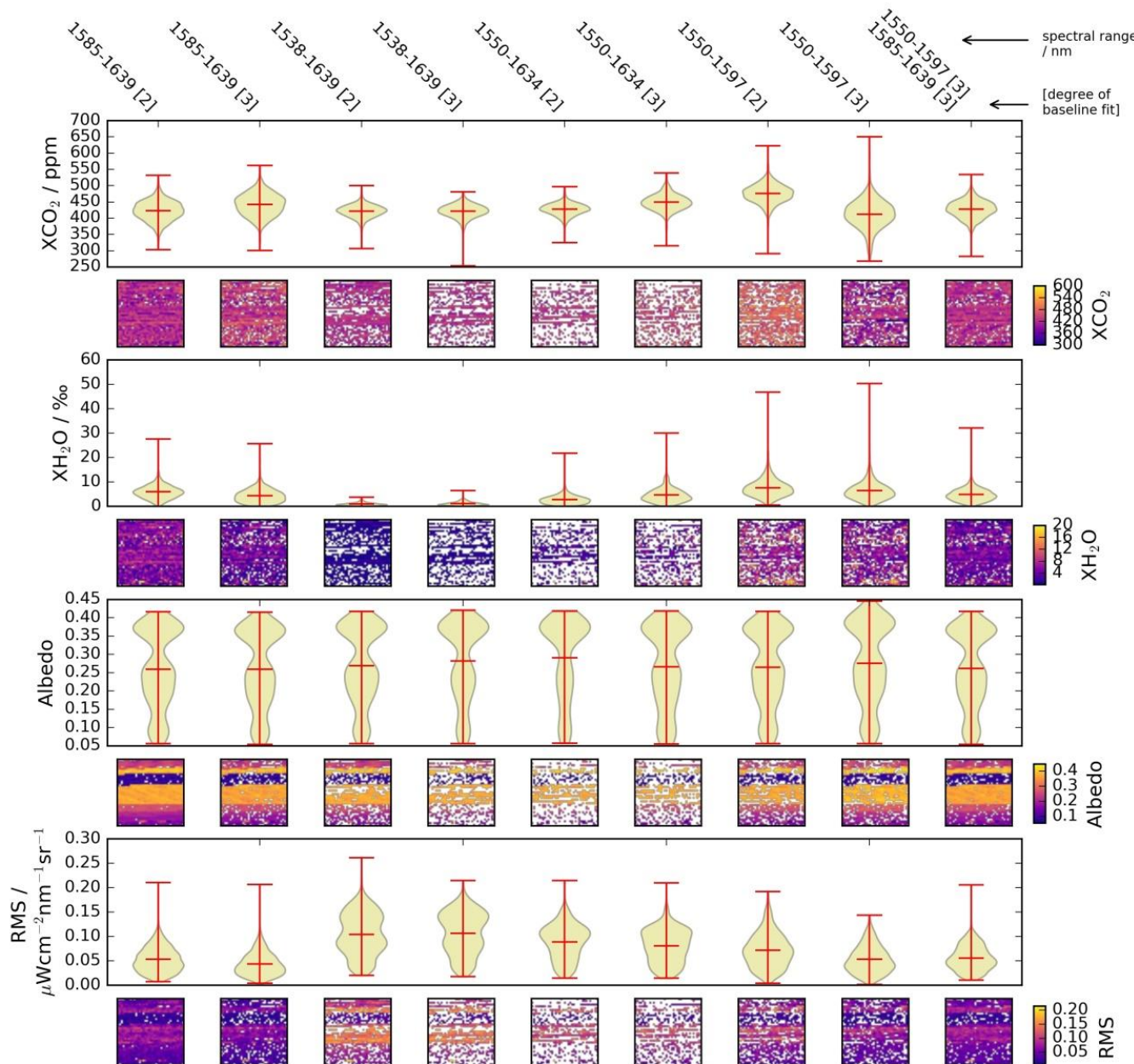


XCO₂ retrievals in the SWIR-1 spectral range

- Retrievals conducted with test ensemble using various spectral windows and either a linear or quadratic polynomial baseline fit
- Average convergence rate in SWIR-1 tests: 67%
- Large scatter in XCO₂ ($\sigma_{avg.}=6\%$), XH₂O ($\sigma_{avg.}=54\%$)
- Large spectral residuals observed



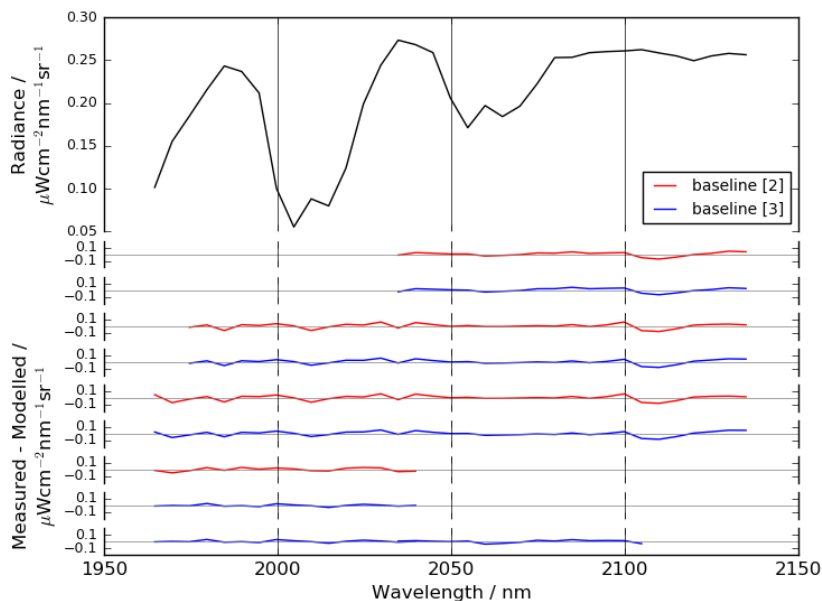
Spectral residuals averaged for all spectra that converged in the test ensemble retrieval. Large, systematic structures here are independent of the underlying spectroscopic database (i.e. HITRAN08 or HITRAN16).



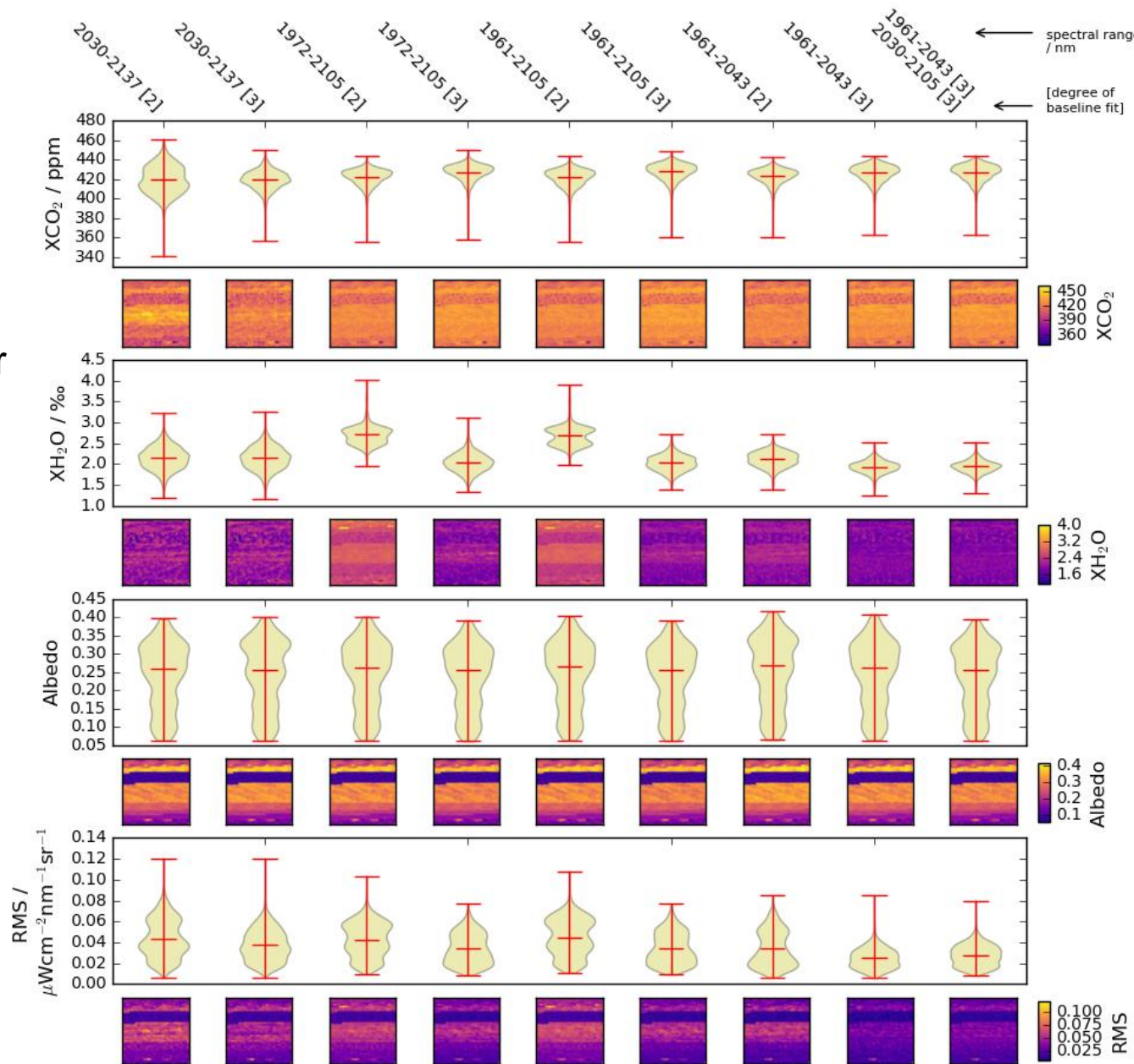
The violin plots show distributions of critical retrieval parameters for various spectral windows (labeled on top). Colored squares show images of retrieval variables (the test ensemble contains 1,369 = 37x37 spectra). White dots represent spectra that did not converge in the retrieval.

XCO₂ retrievals in the SWIR-2 spectral range

- Enhanced convergence rate (100 %)
- Lower XCO₂ ($\sigma_{avg.}=2\%$) and XH₂O ($\sigma_{avg.}=10\%$) scatter
- Strong XCO₂, XH₂O correlation with albedo, baseline (albedo) polynomial fit impacts trace gas distributions
- Large spectral residuals primarily beyond 2,100 nm



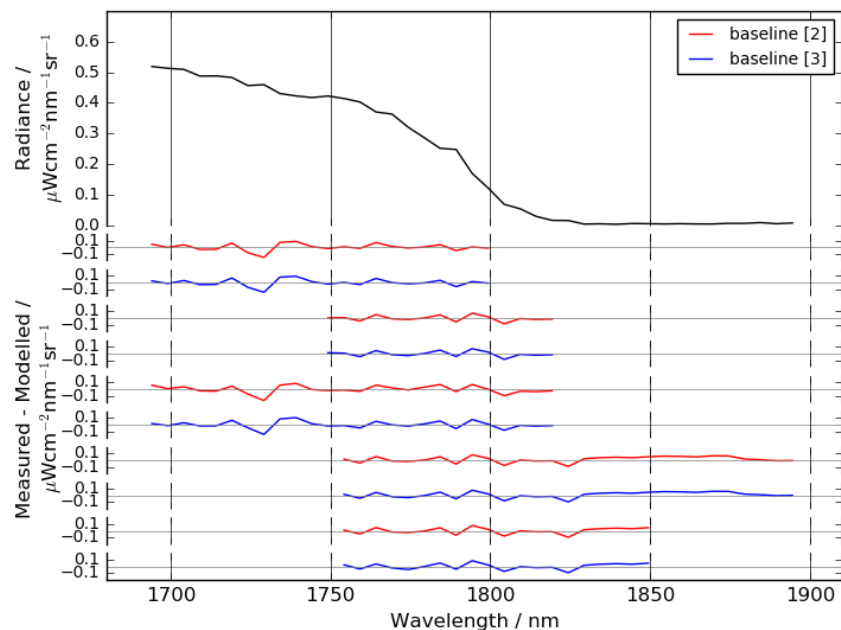
Spectral residuals averaged for all spectra that converged in the test ensemble retrieval. Large, systematic structures here are independent of the underlying spectroscopic database (i.e. HITRAN08 or HITRAN16).



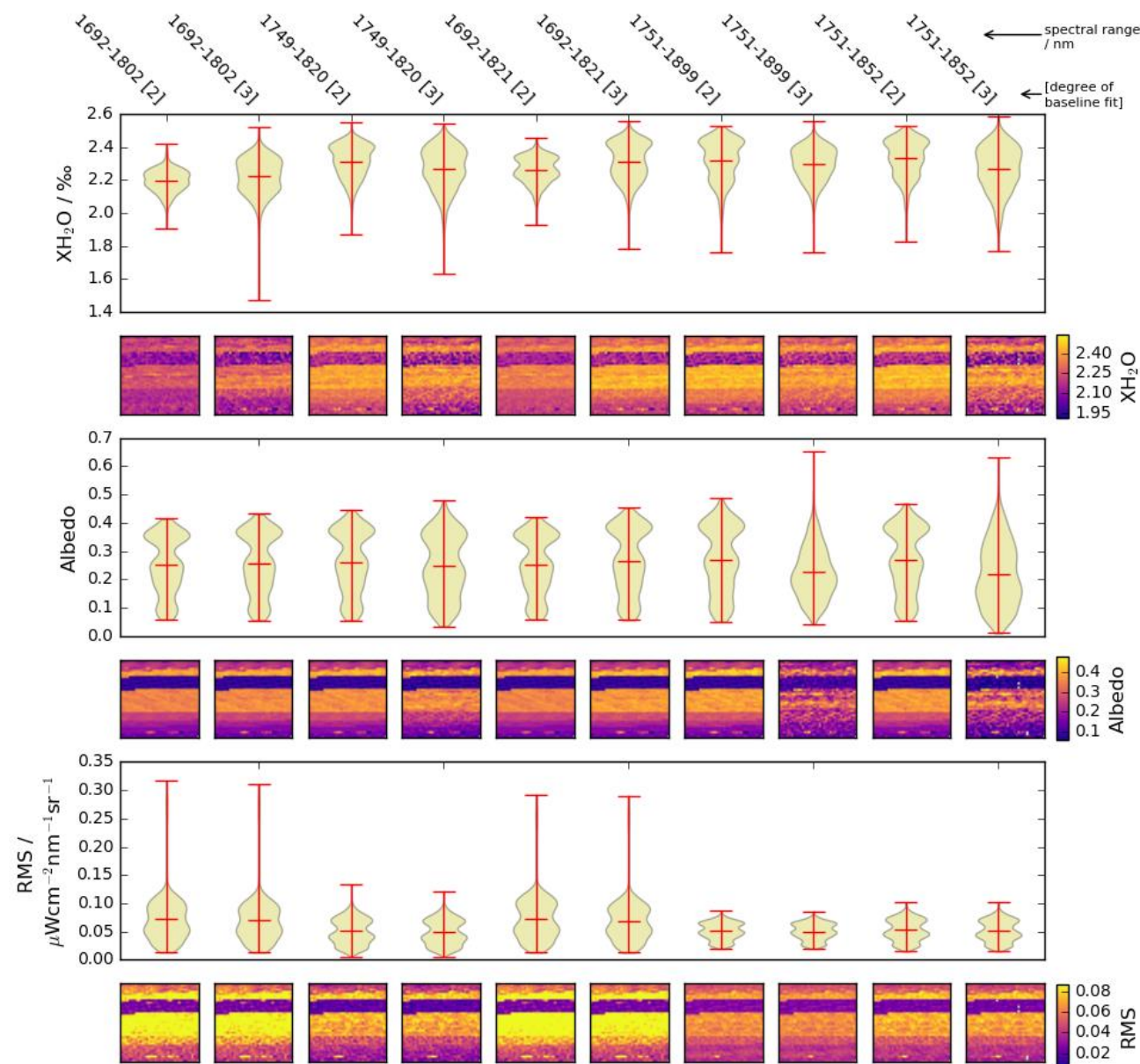
The violin plots show distributions of critical retrieval parameters for various spectral windows (labeled on top). Colored squares show images of retrieval variables (the test ensemble contains 1,369 = 37x37 spectra).

Dedicated water vapor retrieval at 1.8 μm

- Additional spectral window with strong water absorption features to better constrain XH_2O
- Linear baseline fits lead to narrower XH_2O distributions
- Large residuals at 1,720 nm and beyond 1,850 nm should be avoided



Spectral residuals averaged for all spectra that converged in the test ensemble retrieval. Large, systematic structures here are independent of the underlying spectroscopic database (i.e. HITRAN08 or HITRAN16).



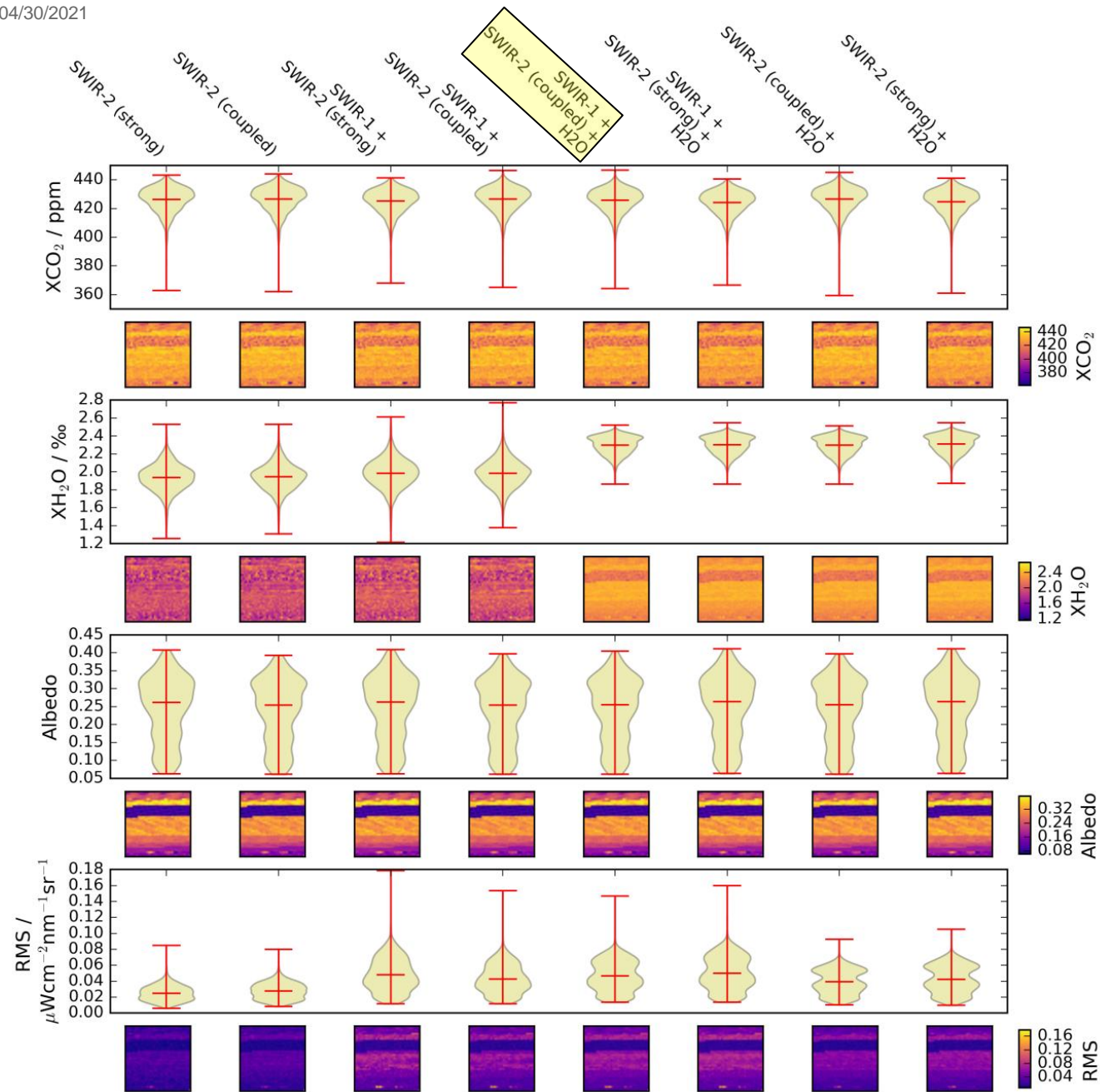
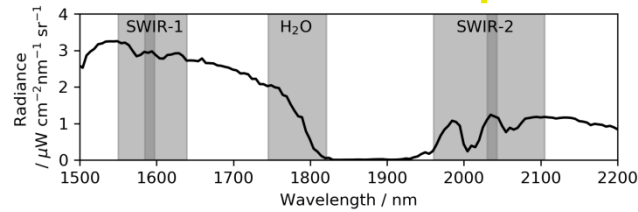
The violin plots show distributions of critical retrieval parameters for various spectral windows (labeled on top). Colored squares show images of retrieval variables (the test ensemble contains 1,369 = 37x37 spectra).

Retrievals with coupled spectral windows

- [H₂O] and [CO₂] coupled between separate retrieval windows
- Several configurations with favorable retrieval performance exist
- Trace gas amounts and surface albedo cannot be detrended in the retrieval

Retrieval Configuration	\bar{X}_{CO_2} / ppm	$\sigma(X_{CO_2})$ / ppm	\bar{X}_{H_2O} / ‰	$\sigma(X_{H_2O})$ / ‰	$R_{ALB}^{H_2O}$	$R_{ALB}^{CO_2}$	σ_{RMS} / Radiance
SWIR-2 (strong)	426.26	8.74	1.94	0.15	0.25	0.71	0.025
SWIR-2 (coupled)	426.60	8.75	1.94	0.15	0.27	0.71	0.028
SWIR-1 + + SWIR-2 (strong)	425.14	8.32	1.98	0.16	0.32	0.69	0.048
SWIR-1 + + SWIR-2 (coupled)	426.59	8.46	1.99	0.16	0.37	0.69	0.043
SWIR-1 + H ₂ O + + SWIR-2 (coupled)	425.68	8.33	2.30	0.10	0.91	0.69	0.046
SWIR-1 + H ₂ O + + SWIR-2 (strong)	424.21	8.27	2.30	0.10	0.91	0.69	0.050
SWIR-2 (coupled) + + H ₂ O	426.50	8.64	2.30	0.10	0.91	0.72	0.039
SWIR-2 (strong) + + H ₂ O	424.81	8.60	2.31	0.10	0.91	0.71	0.042

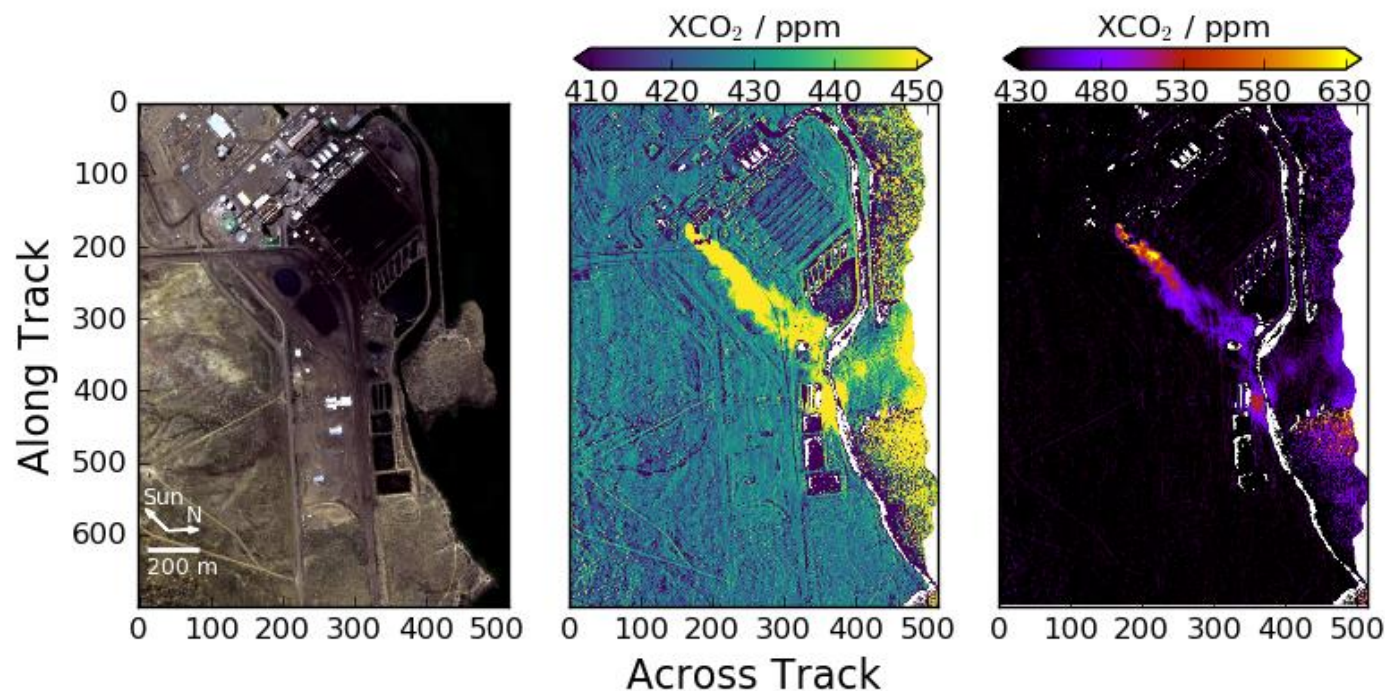
These spectral windows used for power plant XCO₂ plume retrievals



Comparison of retrievals with spectral windows coupled across the SWIR range. The configuration marked in yellow uses an individual spectral window for each of the four CO₂ bands and an extra H₂O window.

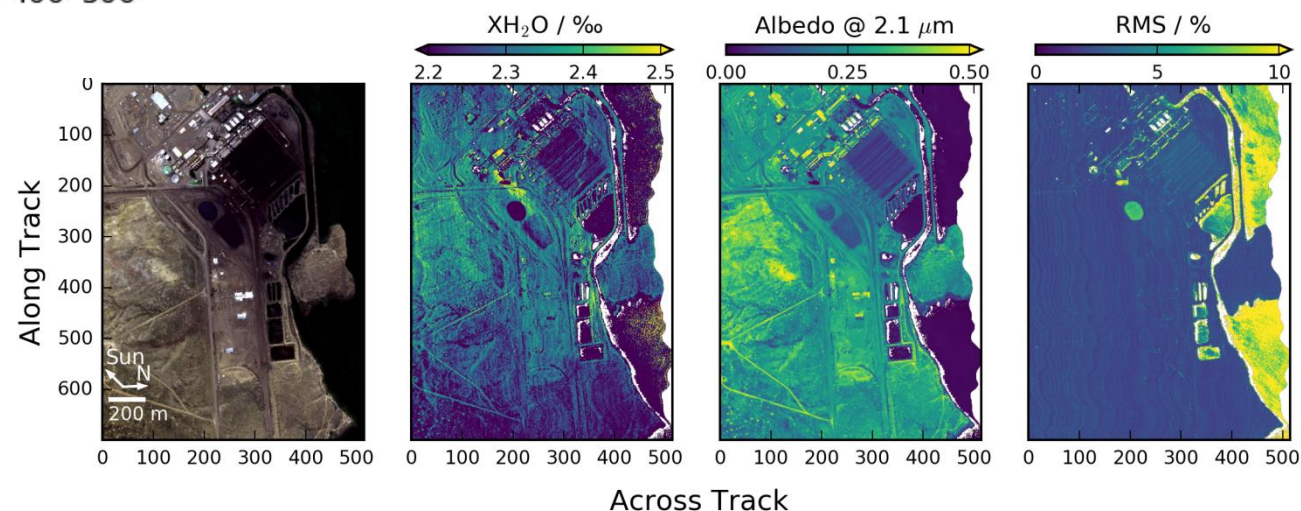
Retrieval performance data for the most promising configurations. \bar{X} signifies average value, σ is standard deviation and R denotes the correlation coefficient between two variables.

Retrieval of XCO₂ plume at Four Corners power plant

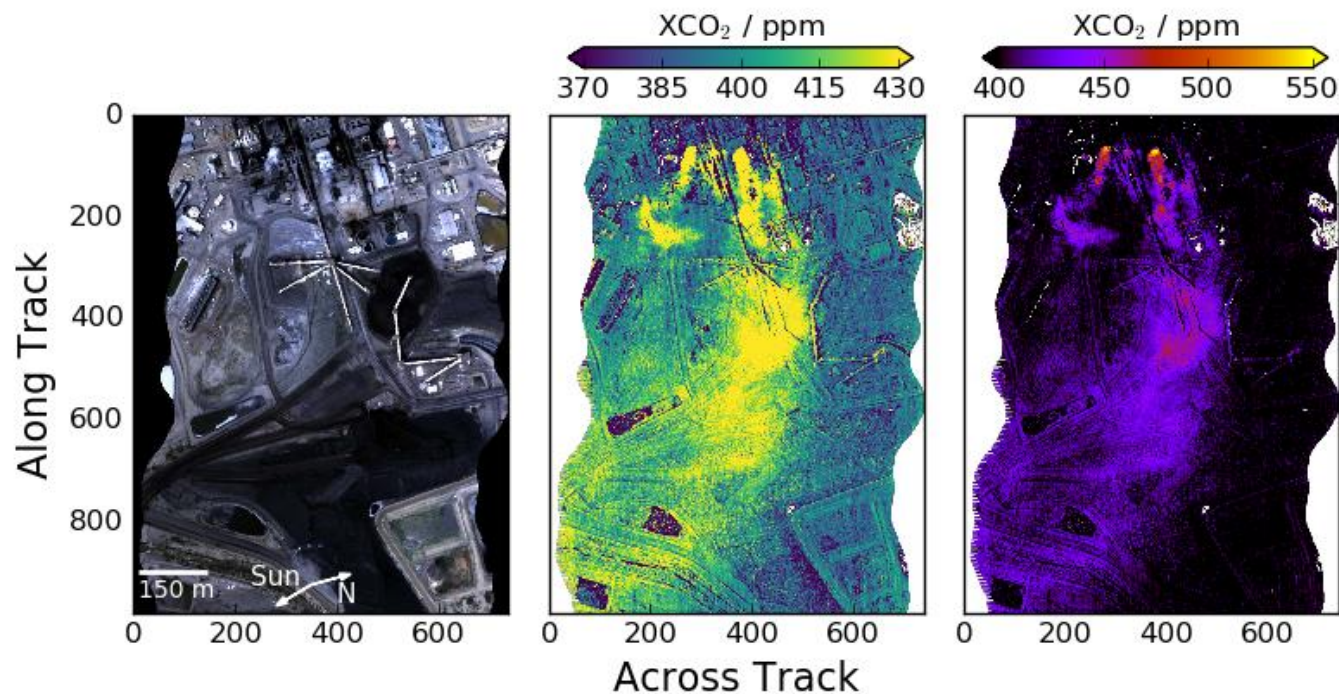


- White pixels: non-convergence of retrieval
- Internal plume structure resolved, large enhancements
- Correlation between XCO₂ and surface albedo remains

- XH₂O retrieval shows exhaust plume and albedo correlation
- Spectral RMS error increased over water surfaces and anthropogenic structures

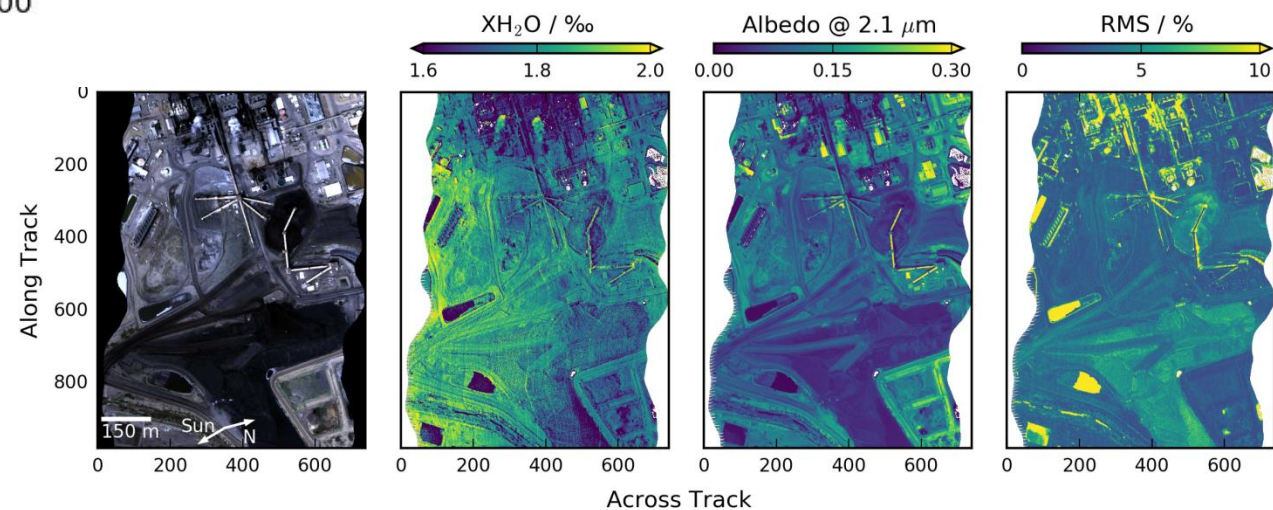


Retrieval of XCO₂ plumes at San Juan power plant



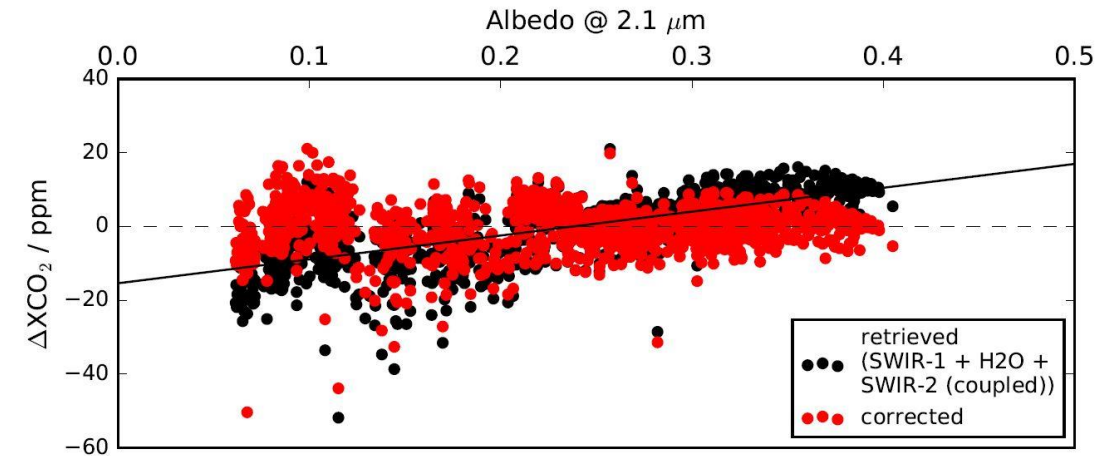
- Two plumes with different wind directions (as observed by [Thorpe et al. \(2017\)](#))
- Condensate emerging from the two stacks
- Pronounced albedo bias

- Water vapor plume coexists with visible condensate (but not beyond)
- Spectral RMS error increased over water surfaces, anthropogenic structures and shadow



Albedo Bias Correction

- Strong albedo bias: apply a linear posterior correction, derived from test ensemble retrievals.
- Dark scenes ($\text{albedo}_{@2.1\mu\text{m}} < 0.03$) removed as XCO_2 retrieval scatter is unrealistically high
- The correction
 - Reduces the XCO_2 -albedo correlation coefficient to below 0.25 in background scenes of both power plant flights.
 - Reduces the XCO_2 background retrieval standard deviation by ~ 1 ppm in both scenes.



Linear (posterior) bias correction for XCO₂ retrievals of the ensemble of test spectra.

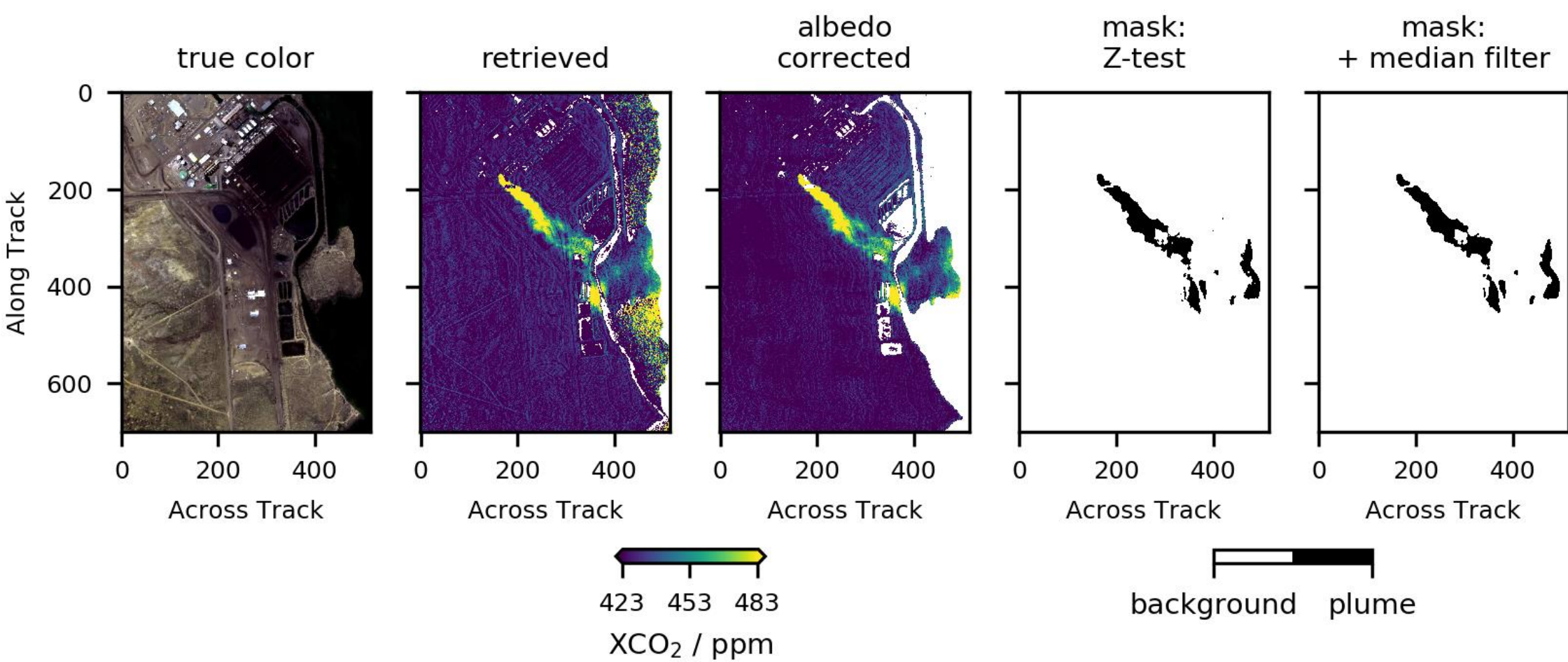


Plume mask for Four Corners scene

- Plume masking procedure inspired by [Varon et al. \(2018\)](#)

$$Z = \frac{XCO_2 - XCO_2^{bg}}{2\sigma_{bg}} > 0.95$$

Smooth with median of 5x5 pixel neighborhood

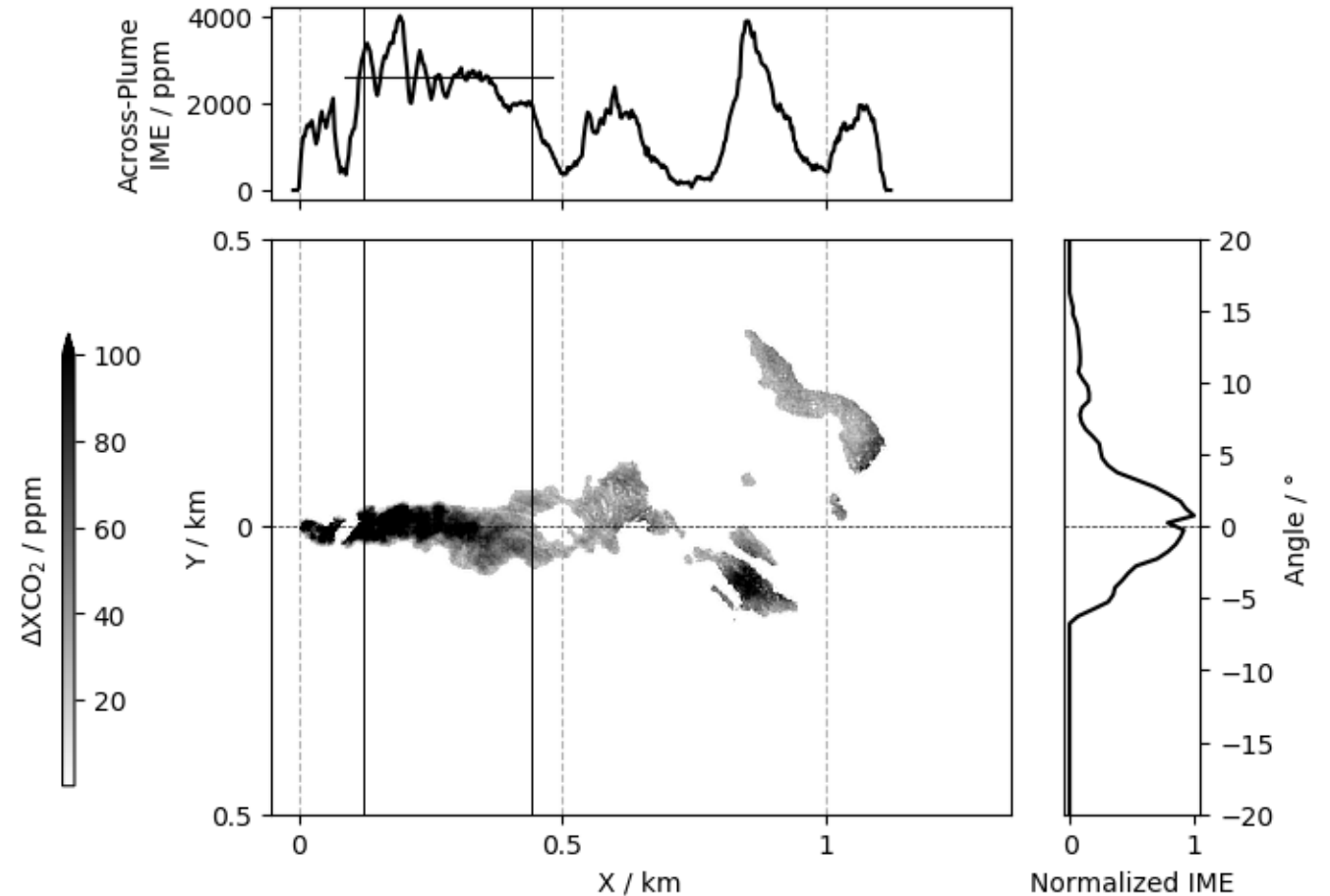


→ Plume is cut off by sensor swath and obstructed by water surfaces → mass balance flux inversion

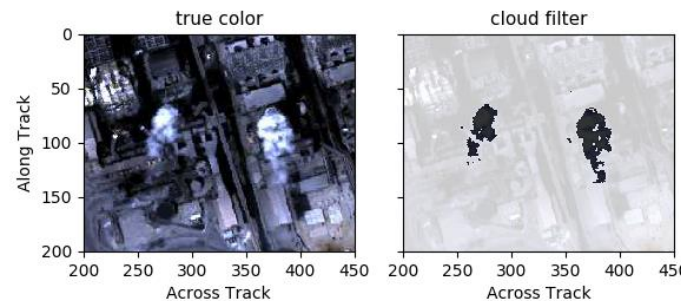


Plume morphology of Four Corners scene

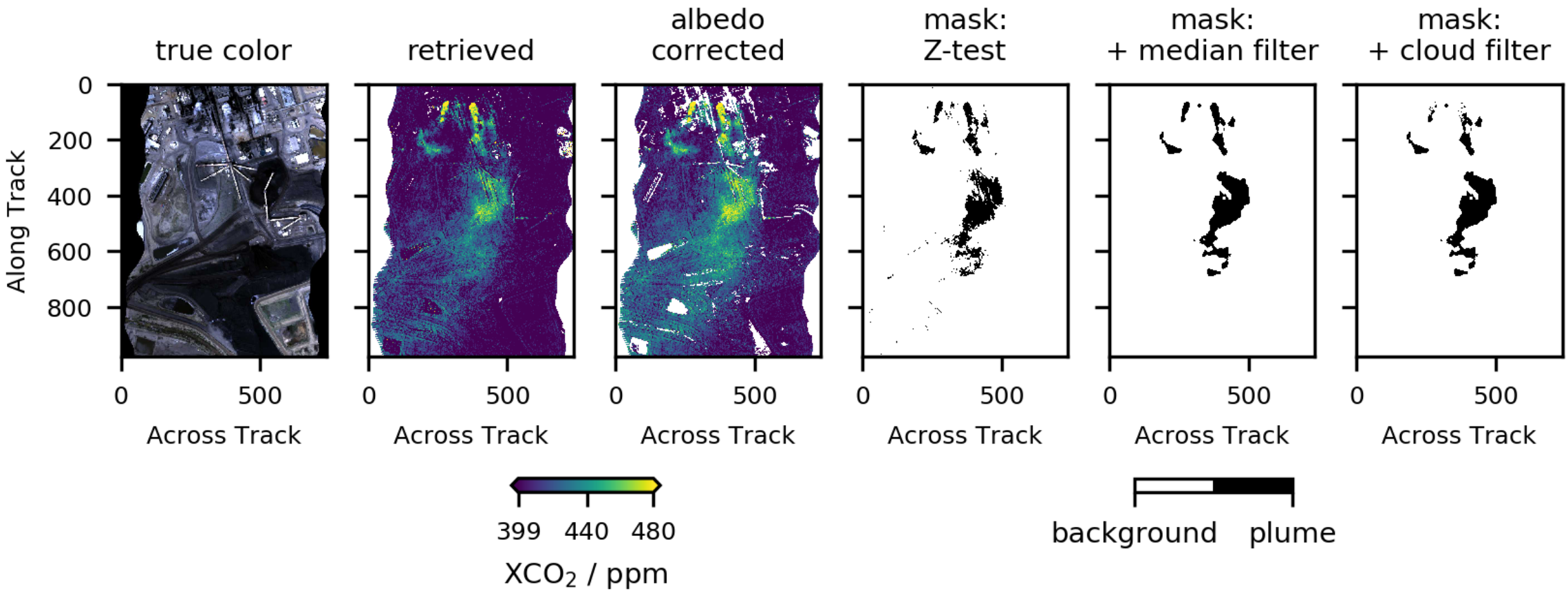
- Plume rotated around its major axis
- Individual turbulent eddies resolved
- Narrow angular distribution indicates high wind speed (as discussed by [Jongaramrungruang et al. 2019](#))
- Across-plume mass enhancement calculated from an average over a contiguous plume area



Plume mask for San Juan scene



Simple radiance filter for clouds:
 $I_{1,548 \text{ nm}}/I_{2,054 \text{ nm}} + I_{502 \text{ nm}} > 11 \mu\text{W sr}^{-1}\text{cm}^{-2}\text{nm}^{-1}$



→ No major missing plume areas → integrated mass enhancement (IME) flux inversion



Emission rate estimates

- Stack heights are 116 m (Four Corners) and 122 m (San Juan)^[5].
- ECMWF ERA5 reanalyses are substantially low-biased near the two power plant stacks. The same bias was observed by [Borchardt et al \(2021\)](#) in the Four Corners region.
- NCEP NARR^[8] 30 m wind speeds agree better with the observed plume shapes → use NARR data
- Mass balance method used for Four Corners scene
- Integrated mass enhancement method for San Juan scene
- Wind speed uncertainty conservatively estimated at 3 m/s for both scenes.

Wind speed source	Wind speed @ 4Corners [m/s]	Wind speed @ San Juan [m/s]
ECMWF ERA5 ^[6] interpolated at stack altitude; $\Delta t=1h$	0.6	1.2
Surface measurement @ nearby airport ^[7] ; $\Delta t=2h$, $\Delta x \approx 25km$	7.5	3.1
NCEP NARR ^[8] interpolated at 30 m above ground; $\Delta t=3h$	6.1	4.3

	Q (4Corners) / MtCO ₂ y ⁻¹	Q (San Juan) / MtCO ₂ y ⁻¹
Present study	17.4 ± 8.8	17.8 ± 14.1
EPA inventory ^[9]	8.8	9.9



Summary and Conclusions

- XCO₂ retrievals from AVIRIS-NG spectra perform best when strong absorption bands of CO₂ and H₂O are included in the spectral fitting windows (i.e. CO₂ bands in SWIR-2, wing of opaque H₂O band at 1.8 μm).
- All retrieval set-ups studied here lead to significant correlation between trace gas columns and surface reflectance: this may be an inherent property of the $\Delta\lambda \sim 5$ nm resolution of the sensor.
- Fitting individual CO₂ absorption bands in separate spectral windows is beneficial to reduce spectral residuals.
- The retrieval conducted in this work uses all four CO₂ absorption bands in the SWIR and an extra spectral window at 1.8 μm to constrain XH₂O.
- A posterior (linear) albedo bias correction was applied to detrend XCO₂ from ground albedo.
- Emission rates of power plants critically depend on appropriate wind speed information at the height of the stacks; meteorological reanalyses have to be used with caution.
- Future work should derive wind speed information from the shape of the plume.



References

- [1] <https://avirisng.jpl.nasa.gov/>
- [2] <https://avirisng.jpl.nasa.gov/dataportal/>
- [3] Butz et al., Appl. Opt. (2009)
- [4] Butz et al. GRL (2011)
- [5] <https://dukespace.lib.duke.edu/dspace/handle/10161/407>
- [6] <https://www.ecmwf.int/en/forecasts/datasets/reanalysis-datasets/era5>
- [7] <https://www7.ncdc.noaa.gov/CDO/cdoselect.cmd?datasetabbv=SUMMARIES&countryabbv=&georegionabbv=&resolution=0>
- [8] <https://psl.noaa.gov/data/gridded/data.narr.html>
- [9] <https://ghgdata.epa.gov/ghgp/main.do>

